ISIJ International, Vol. 38 (1998), No. 3, pp. 310–315

In-situ Joining of Nickel Monoaluminide to Iron by Reactive Sintering

Kiyotaka MATSUURA, Kenichi OHSASA,[1] Noritoshi SUEOKA[2] and Masayuki KUDOH

Division of Materials Science and Engineering, Graduate School of Engineering, Hokkaido University, Kita-ku, Sapporo, Hokkaido, 060-8628 Japan. 1) Division of Molecular Chemistry, Graduate School of Engineering, Hokkaido University, Kita-ku, Sapporo, Hokkaido, 060-8628 Japan. 2) Graduate Student, Graduate School of Engineering, Hokkaido University, Kita-ku, Sapporo, Hokkaido, 060-8628 Japan.

(*Received on September 3, 1997; accepted in final form on November 12, 1997*)

A cylindrical block of nickel monoaluminide, NiAl, is produced from a mixture of nickel and aluminum powders by sintering a powder compact under a pseudo-isostatic pressure, and is simultaneously joined to an iron block with the same shape. When the joining couple of the powder compact and the iron block is heated to approximately 900 K, a violent exothermic synthesis reaction, Ni + Al → NiAl, suddenly starts, and the temperature of the compact quickly rises owing to the heat of reaction and exceeds the melting point of NiAl, 1 911 K. Because the molten NiAl wets the contacting surface of the iron block, an iron-rich NiAl-base alloy and an iron-base ternary solid solution are produced on each side of the joining interface. No cracks or cavities are formed in the NiAl even in the vicinity of the joining interface. Hardness continuously changes across the joining interface from approximately 330 in NiAl to approximately 55 in iron. All of five specimens of a four-point bending test fractured in NiAl, the fracture surface being 1 to 2 mm away from the joining interface.

KEY WORDS: powder metallurgy; reactive sintering; combustion synthesis; intermetallic compound; nickel monoaluminide; joining; mechanical property.

1. Introduction

An intermetallic compound of nickel monoaluminide, NiAl, offers new opportunities for developing low-density and high-strength structural materials which might be used at temperatures higher than currently possible with conventional nickel-base superalloys, because NiAl has the attractive combinations of low density (5.86 Mg/m^3), high melting temperature (1 911 K), high strength, good corrosion and oxidation resistance, high thermal conductivity and low cost.[1] Although the most significant disadvantage of NiAl is brittleness at low temperatures, the ductility can be improved by alloying[2] or grain refinement.[3] When NiAl or NiAl-base alloys come in practice in the near future, it becomes necessary to join them to conventional metal materials such as steels or superalloys. However, the joining technique of NiAl has not yet been established.

The present authors[4–11] have studied the synthesis of intermetallics such as NiAl or $MoSi_2$ by reactive sintering or self-propagating high-temperature synthesis (SHS) or, more simply, combustion synthesis, and found that the increase in pressure applied during the reactive sintering reduces the volume fraction of pores remaining in the synthesized intermetallics and that the addition of ceramic particles to the mixture of elemental powders reduces the grain size of the synthesized intermetallics. Throughout our previous study, we have considered that when a compact of the powder mixture being in contact with a metal block is reactive-sintered, the surface layer of the metal block might melt due to the heat of the exothermic reaction of the synthesis, and therefore, the synthesized intermetallic might be joined to the metal block. In this study, we examine the feasibility of the *in-situ* joining of NiAl to an iron block by reactive sintering.

2. Method

2.1. Experiment

Carbonyl nickel powder (99.8 mass% pure, 5 μm in diameter) and gas-atomized aluminum powder (99.8 mass%, 100 μm) were mixed in a molar ratio of 1 : 1 with the addition of small amount of ethanol. The powder mixture was cold-pressed into a cylindrical compact in a metal mold by applying a uniaxial pressure of 600 MPa. The diameter of the compact was 24 mm, and the height was 15 mm. The compact was placed on an iron block with the same shape and size. The contacting surface of the iron block had been polished before hand by using a 400-grit emery paper. The chemical composition of the iron is: C = 0.001, Si = 0.008, Mn < 0.01, P = 0.002, S = 0.001 mass%.

A thermocouple well (3.5 mm in diameter) was drilled

from the top surface of the compact, and two other wells with different depth were drilled from the bottom surface of the iron block, to measure the temperature in the center of the compact and that of the iron block at two different distances from the contacting surface. Type B thermocouples (0.5 mm in diameter) covered with alumina tubes (3 and 2 mm in outer and inner diameters) were inserted into the wells.

Molybdenum wire (0.5 mm in diameter) was wound on to the side surface of the joining couple of the compact and the iron block, and then the joining couple was placed in a pressing vessel (50 mm in inner diameter and 80 mm in depth). The joining couple was pseudo-isostatically pressed at a pressure of 150 MPa through a pressing medium of alumina powder (0.5 mm in diameter), and was then heated at a nominal heating rate of 1 K/s by applying electric power to the molybdenum wire. The pressing and heating were carried out in an evacuated chamber. The sample was removed from the pressing vessel after a period of 300 s passed from the onset of the exothermic reaction of the synthesis, which had been monitored through a sudden increase in temperature.

The samples were metallographically examined by using an optical microscope and a scanning electron microscope. An electron probe microanalyzer was used to determine the nature and distribution of the phases appearing in the sample. A Vickers microhardness tester with an applied load of 0.245 N was used to investigate the hardness distribution across the joining interface. A four-point bending test was carried out at room temperature to estimate the joining strength.

2.2. Numerical Analysis

The heat generation and heat transfer during the reactive sintering of the joining couple were calculated by using Eq. (1).

$$\frac{\partial T}{\partial t}=\alpha\left(\frac{\partial^2 T}{\partial r^2}+\frac{1}{r}\frac{\partial T}{\partial r}+\frac{\partial^2 T}{\partial z^2}\right)+\frac{\Delta H}{C}\left(\frac{df}{dt}\right)(1-f) \quad \text{.....(1)}$$

The reaction rate of the synthesis, df/dt in Eq. (1), was assumed to be expressed as the following form[12]

$$\frac{df}{dt}=A\exp(-Q/RT) \quad \text{.....(2)}$$

The value of A in Eq. (2) was determined empirically so as to reproduce reasonably the time–temperature curves obtained in this study. The boundary conditions are:

$$\frac{\partial T}{\partial r}=0 \quad (\text{at } r=0) \quad \text{.....(3)}$$

$$\lambda_{\mathrm{NiAl}}\frac{\partial T}{\partial z}=\lambda_{\mathrm{Fe}}\frac{\partial T}{\partial z}=h_1(T_{\mathrm{m}}-T_{\mathrm{F}}) \quad (\text{at } z=z_1) \quad \text{....(4)}$$

$$\lambda_{\mathrm{NiAl}}\frac{\partial T}{\partial r}=\lambda_{\mathrm{Fe}}\frac{\partial T}{\partial r}=-h_{\mathrm{S}}(T_{\mathrm{S}}-T_{\mathrm{A}}) \quad (\text{at } r=r_{\mathrm{S}}) \quad \text{....(5)}$$

$$\lambda_{\mathrm{Fe}}\frac{\partial T}{\partial z}=-h_{\mathrm{S}}(T_{\mathrm{S}}-T_{\mathrm{A}}) \quad (\text{at } z=0) \quad \text{.....(6)}$$

Table 1. Properties used in the numerical analysis.[13–16]

Property	Value
C_{Fe} (kJ/(kg·K))	0.65
C_{NiAl} (kJ/(kg·K))	$0.53+0.00023T$[14]
λ_{Fe} (W/(m·K))	28.4
λ_{NiAl} (W/(m·K))	75.2[15]
ρ_{Fe} (Mg/m^3)	7.8
ρ_{NiAl} (Mg/m^3)	5.9[14]
L_{Fe} (kJ/kg)	268
L_{NiAl} (kJ/kg)	200[14]
h_{I} (W/(m^2·K))	5 000[13]
h_{S} (W/(m^2·K))	420
A (s^{-1})	5.5×10^8
Q (kJ/mol)	146.3[16]
ΔH (kJ/kg)	1 380[14]

$$\lambda_{\mathrm{NiAl}}\frac{\partial T}{\partial z}=-h_{\mathrm{S}}(T_{\mathrm{S}}-T_{\mathrm{A}}) \quad (\text{at } z=z_{\mathrm{C}}) \quad \text{.....(7)}$$

In order to solve Eqs. (1) through (7) numerically by using a finite difference method, the longitudinal cross section of the sample was divided into 3 600 rectangular grids with sides 0.25 and 0.5 mm on the r- and z-coordinates, and Eq. (1) and Eqs. (3) through (7) were converted into finite difference equations. The time step was 0.00125 s. The ambient temperature was elevated at a rate of 1 K/s, and the temperature of each grid at every time step was calculated. It was assumed that when the temperature of a grid reached 900 K, the synthesis reaction proceeded at the rate described in Eq. (2). The values of various physical properties used in this calculation are given in **Table 1**.

3. Results and Discussion

3.1. Heat Generation and Heat Transfer

Figure 1 shows the results of temperature measurement at three different points in the joining couple. When the joining couple is heated to approximately 900 K, the temperature of the compact suddenly rises as a result of the exothermic reaction of the synthesis of NiAl (see Curve A), and the heat of the reaction is transferred from the compact to the iron block (see Curves B and C). The maximum temperature of the compact is approximately 1 900 K, which is very close to the melting point of NiAl, 1 911 K. The maximum temperature of the iron block reaches approximately 1 300 K even in the center of the thickness of 15 mm.

Figure 2 shows the simulated time–temperature curves at several points on the longitudinal axis of the joining couple. The temperature of the compact exceeds the melting point of NiAl by approximately 300 K in the center (see Curve A) and approximately 200 K even at the joining interface (see Curve D), which indicates that nickel and aluminum powders exothermically react and produce molten NiAl. The temperature of the molten NiAl quickly falls and stagnates for a moment at the freezing point of NiAl, and then gradually falls again. The curves for the temperature of the iron block agree with the experimental results shown in Fig. 1, both at 2 and at 7 mm from the joining interface (Curves B and

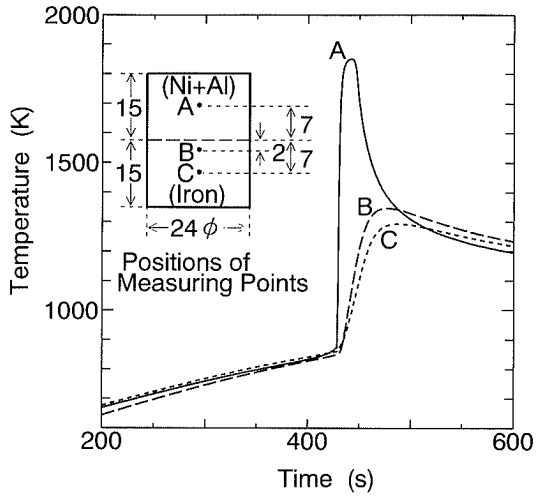

Fig. 1. Measured time–temperature curves of the joining couple.

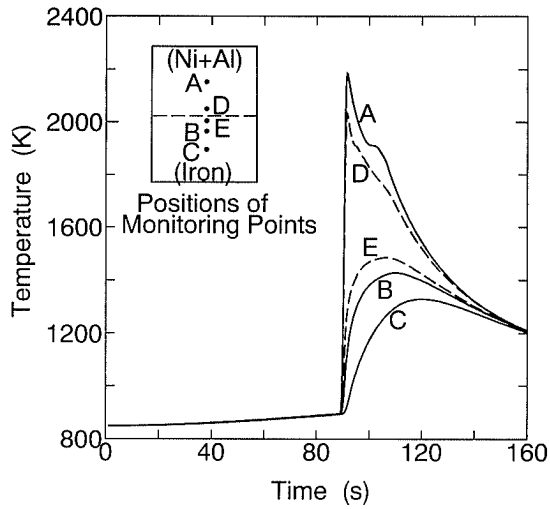

Fig. 2. Simulated time–temperature curves of the joining couple.

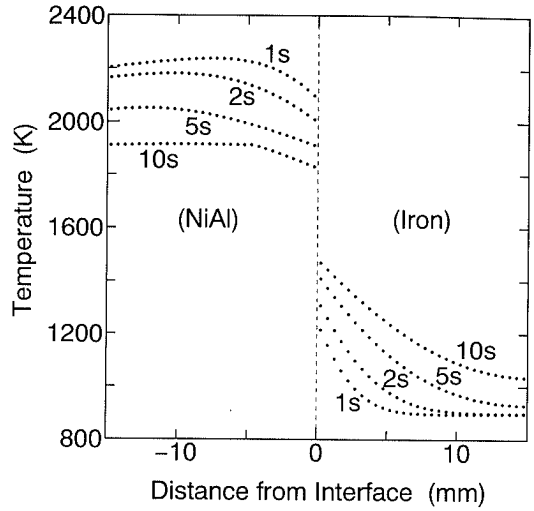

Fig. 3. Simulated temperature distribution curves on the longitudinal axis of the joining couple at several moments from the onset of the synthesis reaction.

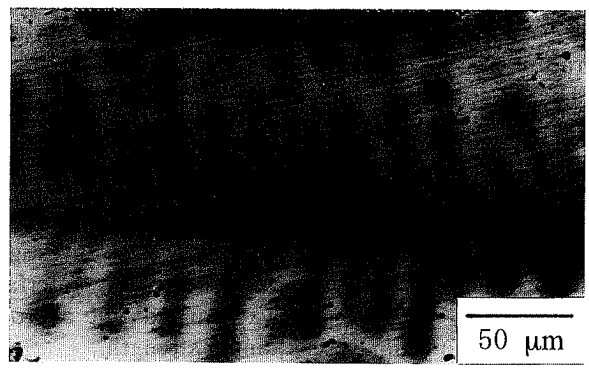

Fig. 4. Microstructure of the synthesized NiAl, showing columnar dendrites. Etchant: Marble's reagent.

C). The temperature of the iron block at the joining interface rises to a higher level than at other two positions (see Curve E), but it does not reach the melting point of iron, 1 811 K, which indicates that the surface of the iron block does not melt, even if the heat of the violent exothermic reaction is transferred to the iron.

Figure 3 shows the simulated temperature distribution curves on the longitudinal axis of the joining couple at several moments from the onset of the synthesis reaction. At a moment of 1 s from the onset, the temperature of the compact exceeds the melting point of NiAl at any position. Heat flows out of the molten NiAl mainly into the iron block: the temperature of the NiAl falls and stagnates for a moment at the freezing point of NiAl, while the temperature of the iron block gradually rises. After the stagnation at the freezing point, the temperature drop of the NiAl begins at the joining interface, which may bring about the directional solidification of the NiAl.

3.2. Metallography

Figure 4 shows the microstructure of the synthesized NiAl. The dendrite structure in the figure indicates that the compact was melted by the heat of the exothermic reaction. The microstructure shown in Fig. 4 supports the simulated results shown in Figs. 2 and 3, and implies that the measured temperatures shown in Fig. 1 were underestimated probably due to the thermal capacity of the alumina tube covering the thermocouple. The columnar shape of the dendrites is a result of the directional solidification, as described in the final part in Sec. 3.1.

Figure 5 shows the microstructure of the joining couple photographed by using a scanning electron microscope. The structure of the synthesized NiAl is uniform, and no defects such as cracks or cavities are observed in the NiAl even at the joining interface, which indicates that the *in-situ* joining of NiAl to the iron block by reactive sintering is feasible. It was considered that because the thermal expansion coefficient of NiAl is very close to that of iron,[17] cracking did not occur during cooling after the *in-situ* joining. However, it was also considered that tensile stress should have generated in NiAl due to the expansion of iron caused by the austenite-to-ferrite transformation during cooling, but no cracks were observed at the joining interface. In the next paragraph, we discuss the reason for the excellent joining property

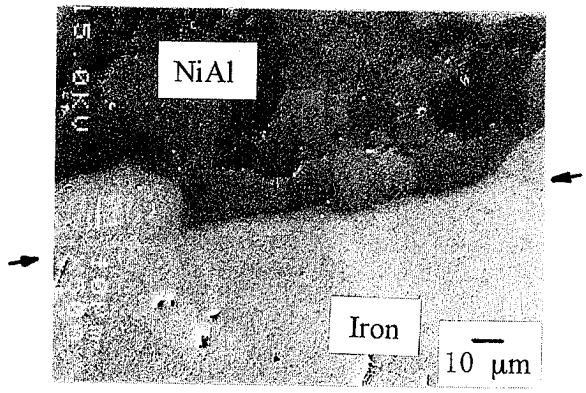

Fig. 5. Microstructure of the joining couple photographed by using a scanning electron microscope. Arrows indicate the joining interface.

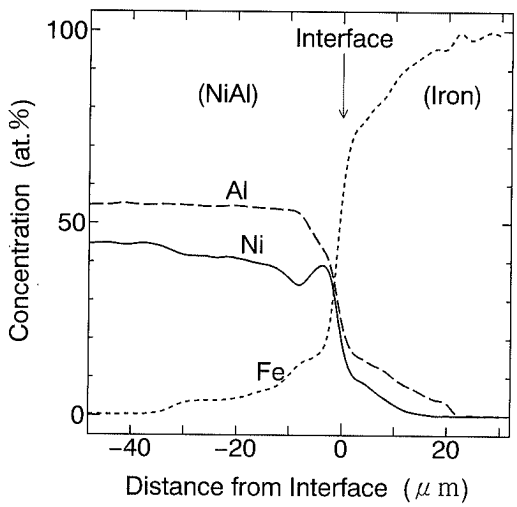

Fig. 6. Concentration distributions of nickel, aluminum and iron across the joining interface.

without cracks, by using the results of chemical analysis.

Figure 6 shows the concentration distributions of nickel, aluminum and iron across the joining interface. The results indicate that (1) the synthesized NiAl has a chemical composition of approximately 45at%Ni–55 at%Al, (2) iron diffuses into the NiAl, replacing nickel atoms, and (3) both nickel and aluminum diffuse into the iron block. According to a nickel–aluminum–iron ternary phase diagram,[18] β-NiAl stably coexists both with α-iron and with γ-iron. The stable conjugation between β-NiAl and α- or γ-iron is considered to be one reason for the excellent joining property. Another reason may be the existence of a cushioning layer with no or little austenite-to-ferrite transformation near the joining interface. According to the ternary phase diagram, the fraction of austenite (γ-iron) phase in an iron–nickel–aluminum alloy decreases with the increase in aluminum content; no austenite exists at any temperature for an Fe–3at%Ni–10at%Al alloy, for example, which corresponds to the chemical composition of the iron at a position 10 μm away from the joining interface, according to the analysis results shown in Fig. 6. It is considered that the cushioning layer with no or little transformation prevents the stress caused by the transformation from concentrating at the joining interface.

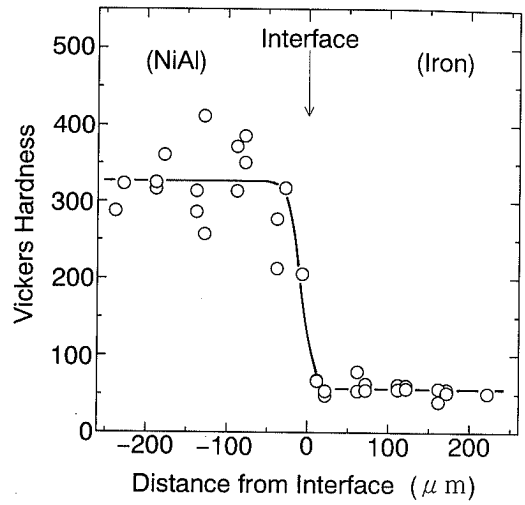

Fig. 7. Hardness distribution across the joining interface.

Because no elemental phases or no intermediate reaction products such as Ni_2Al_3 are observed in Fig. 6, it is shown that the synthesis reaction is completed even in the vicinity of the joining interface, which agrees with the simulated results in Fig. 2 showing that the maximum temperature of the compact exceeds the melting point of NiAl even at the interface. We had considered that a thin layer of the iron at the joining interface might melt due to the heat from the exothermic reaction of the synthesis. However, the simulated results shown in Fig. 2 indicate that the iron block does not melt even at the joining interface. The alloying near the joining interface, both in NiAl and in iron, is considered to have been produced not by mixing of liquids but by diffusion before and after solidification of the molten NiAl.

3.3. Mechanical Properties

Figure 7 shows the hardness distribution across the joining interface. The indentations were made in a zigzag manner to avoid an interaction between the nearest indentations. Hardness changes continuously from high values in the synthesized NiAl to low values in the iron block. The average hardness of approximately 55 in the iron block is considered to be reasonable, based on the chemical composition described in Sec. 2.1. The hardness of the NiAl is approximately 330 on the average, but it varies from 260 to 420. We discuss the reason for the variation in hardness of the NiAl in the next paragraph.

Figure 8 shows the concentration distributions of nickel and aluminum in the synthesized NiAl away from the joining interface. The average composition of the NiAl is approximtely 50at%Ni–50at%Al, but the composition varies with the maximum width of approximately 10 at%, which is within the solubility range of NiAl, according to an aluminum–nickel binary equilibrium phase diagram.[19] The variation in the concentration may be caused by the inhomogeneous mixing of the elemental powders or by the microsegregation during the solidification of the molten NiAl. We have previously investigated the effect of nickel content on the hardness of NiAl, and found that the hardness decreases from 400

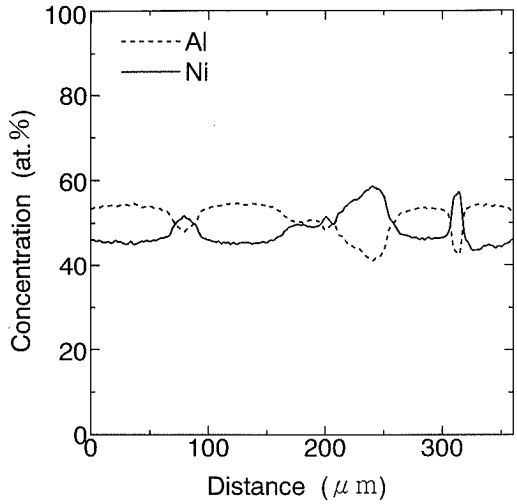

Fig. 8. Concentration distributions of nickel and aluminum in the synthesized NiAl away from the joining interface.

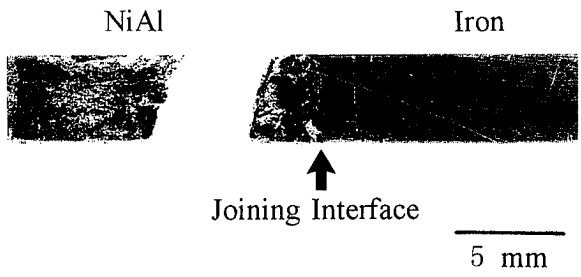

Fig. 9. Fractured specimen of a four-point bending test.

to 300 as the nickel content increases from 46 to 50 at%, but it increases to 400 as the nickel content increases further to 56 at%.[7] Similar results were reported by Westbrook,[20] Nagpal and Baker,[21] and Tan *et al.*[22] According to Bradley and Taylor,[23] NiAl has different types of lattice defects between both sides of the stoichiometric composition; *i.e.* the vacancies at the nickel sites for the aluminum-rich side and the substitutional nickel atoms at the aluminum sites for the nickel-rich side. Tan *et al.* explained the change in hardness of NiAl from the change in lattice parameter. Consequently, the variation in hardness of the NiAl shown in Fig. 7 is caused by the nonuniformity in concentration of nickel and aluminum within the solubility range of NiAl.

Figure 9 shows a fractured specimen of a four-point bonding test. Five samples were tested under the following conditions: $3 \times 4\,mm^2$ in rectangular cross-sectional area, 15 mm in distance between supporting points, 4 mm in distance between loading points and 0.5 mm/min in cross-head speed. Fracture occurred always in the NiAl near the joining interface, as shown in Fig. 9. The crack was propagated both through crystal grains and on grain boundaries, as shown in **Fig. 10**. The fracture strength measured by the bending test was 50 to 60 MPa. The fracture strength may be improved by the addition of alloying elements such as iron or gallium,[24] or by decreasing the porosity in the synthesized NiAl which was estimated to be 2 to 5 vol% in the present samples.

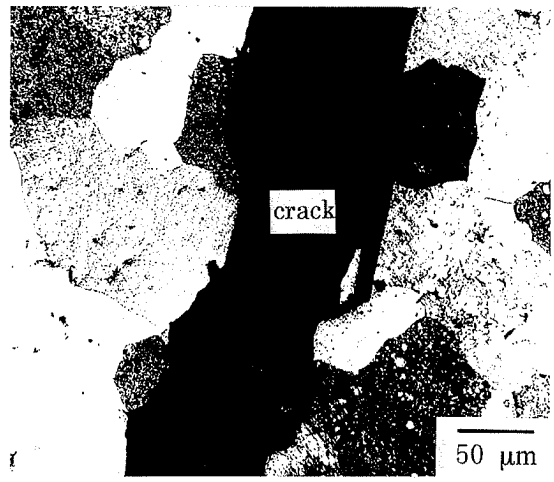

Fig. 10. Crack formed in the NiAl.

4. Conclusions

The joining couple of an iron block and a compact of powder mixture of nickel and aluminum was heated under a pseudo-isostatic pressure, in order to examine the feasibility of an *in-situ* joining of NiAl to iron by reactive sintering. Additionally, a computer simulation was performed by using a finite difference method, in order to simulate the heat generation and heat transfer during the reactive sintering. The results are summarized as follows.

(1) When the joining couple is heated to approximately 900 K, nickel and aluminum suddenly react exothermically, and NiAl is instantly synthesized. The temperature of the compact quickly rises and exceeds the melting point of NiAl, 1911 K. The heat of the reaction enables the *in-situ* joining between the synthesized NiAl and the iron block.

(2) The microstructure of the synthesized NiAl is uniform and there are neither intermediate reaction products such as Ni_2Al_3 nor defects such as cracks or cavities even at the joining interface. During cooling of the molten NiAl, iron defuses into the NiAl, while nickel and aluminum diffuse into the iron block.

(3) Hardness continuously changes across the joining interface from approximately 330 in the NiAl to approximately 55 in the iron block. The fracture strength of the joining couple measured by a four-point-bending test was 50 to 60 MPa. The crack was propagated both through crystal grains and on grain boundaries of NiAl, the fracture surface being 1 to 2 mm away from the joining interface.

Acknowledgement

The authors gratefully acknowledge the financial support from KAWASAKI STEEL 21st Century Foundation.

Nomenclature

A: coefficient related to the reaction mechanism
C: specific heat
f: fraction of the formed NiAl
h_1: heat transfer coefficient at the joining interface

h_S: heat transfer coefficient at the surface of the joining couple
ΔH: heat of formation of NiAl
L: latent heat
Q: activation energy
r: radial coordinate in a cylindrical system
r_C: radius of the joining couple
R: gas constant
t: time
T: temperature
T_A: temperature of the pressing medium
T_F: temperature of the iron at the joining interface
T_m: temperature of the NiAl at the joining interface
T_S: temperature of the surface of the joining couple
z: axial coordinate in a cylindrical system
z_C: height of the joining couple
z_I: position of the joining interface on the z-coordinate
α: thermal diffusivity ($=\lambda/\rho C$)
λ: thermal conductivity
ρ: density

REFERENCES

1) R. Darolia: *J. Met.*, **43** (1991), 44.
2) S. Guha, P. R. Munroe and I. Baker: *Mat. Res. Soc. Symp. Proc.*, **133** (1989), 633.
3) E. M. Schulson and D. R. Barker: *Scr. Metall.*, **17** (1983), 519.
4) K. Matsuura, T. Ohmi, Y. Itoh, M. Kudoh and D. Tanaka: *J. Jpn. Inst. Light Met.*, **45** (1995), 144.
5) K. Matsuura, Y. Itoh and M. Kudoh: Proc. PRICM2, 1 (1995), 395.
6) K. Matsuura, T. Kitamura, M. Kudoh and Y. Itoh: *Mater. Trans. JIM*, **37** (1996), 1067.
7) K. Matsuura, T. Kitamura and M. Kudoh: *J. Jpn. Inst. Light Met.*, **46** (1996), 383.
8) K. Matsuura, T. Kitamura and M. Kudoh: *J. Mater. Process. Technol.*, **63** (1997), 298.
9) K. Matsuura, T. Kitamura, M. Kudoh, Y. Itoh and T. Ohmi: *ISIJ Int.*, **37** (1997), 87.
10) K. Matsuura, T. Ohmi, M. Kudoh, T. Kakuhashi and T. Hasegawa: *J. Jpn. Inst. Light Met.*, **47** (1997), 446.
11) K. Matsuura and M. Kudoh: *J. Mater. Sci. Eng.*, in press.
12) Y. Miyamoto: Nenshougousei-no-Kagaku (Chemistry of Combustion Synthesis), ed. by M. Koizumi, Research Group of Combustion Synthesis, Osaka, (1992), 34.
13) I. Ohnaka: Introduction of Computer Analysis for Heat Transfer and Solidification, Maruzen, Tokyo, (1985).
14) T. A. Mielsen: A Study of Self Propagating High Temperature Synthesis of Nickel Aluminide, Thesis, Wayne States Univ.
15) R. D. Noebe, R. R. Bowman and M. V. Nathal: Physical Metallurgy and Processing of Intermetallic Compounds, ed. by N. S. Stoloff and V. K. Sikka, Chapman and Hall, New York, (1996), 217.
16) T. S. Dyer and Z. A. Munir: *Metall. Trans. B*, **26B** (1995), 603.
17) M. I. Sandakova, V. M. Sandakov, G. I. Kalishevich and P. V. Gel'd: *Russ. J. Phys. Chem.*, **45** (1971), 901.
18) P. Budberg and A. Prince: Ternary Alloys, Vol. 5, ed. by G. Petzow and G. Effenberg, VCH Verlagsgesellschaft, Weinheim, (1993), 309.
19) M. F. Singleton, J. L. Murray and P. Nash: Binary Alloy Phase Diagrams, Vol. 1, ed. by T. B. Massalski, Am. Soc. Met., Materials Park, Ohio, (1990), 181.
20) J. H. Westbrook: *J. Electr. Soc.*, **103** (1956), 54.
21) P. Nagpal and I. Baker: *Metall. Trans. A*, **21A** (1990), 2281.
22) Y. Tan, T. Shinoda, Y. Mishima and T. Suzuki: *J. Jpn. Inst. Met.*, **57** (1993), 220.
23) A. J. Bradley and A. Taylor: *Proc. R. Soc.*, **A159** (1937), 56.
24) R. D. Neobe and M. K. Behbehani: *Scr. Metall. Mater.*, **27** (1992), 1795.